ACS OMEGA

Open Access

This article is licensed under CC-BY-NC-ND 4.0

http://pubs.acs.org/journal/acsodf

Article

Mechanistic Analysis and Process Simulation of Ethyl Acetate-Ethanol Separation by Complex Solvent Extractive Distillation

Jiajie Liu, Yueran Yin, Sijia Dai, Biao Liu, and Qiang Wang*

Cite This: *ACS Omega* 2024, 9, 26596−26606

Read Online

ACCESS | Metrics & More | Article Recommendations | Supporting Information

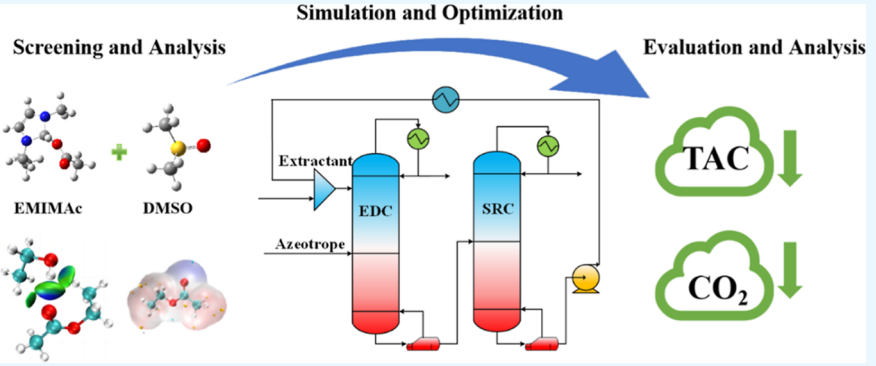

ABSTRACT: Developing high-performance solvents for extraction and optimizing process technologies is crucial for efficient extractive distillation (ED) separation of azeotrope mixtures. In this paper, computer-aided screening was used to study the ED of azeotrope mixtures in ethyl acetate and ethanol systems using organic solvent dimethyl sulfoxide (DMSO) and ionic liquid (IL) ([EMIM][Ac]). The structural relationship between the ILs and the azeotrope mixture was analyzed by σ-profile, molecular surface electrostatic potential, interaction energy, and separation gradient. Subsequently, process simulation was carried out using Aspen Plus software and global optimization was performed with genetic algorithm, which found that both traditional organic solvents and ILs have good separation effects. But considering the high volatility of organic solvents and low saturation vapor pressure of ILs, it is considered to combine them to further explore the cost and carbon emission advantages in extractive distillation separation. Compared with pure organic solvent and pure ILs separation processes, the TAC of the process using an IL-based mixed solvent process decreased by 5.11 and 21.98%, respectively. The carbon emissions of the mixed extractant process were slightly higher than those of the pure organic solvent process, but the addition of ILs made very little volatilization of organic solvents, saving a charge for extractant use. By improving the process, waste heat is effectively recovered, which can save most of the utility engineering costs, and compared with the previous process, the total alkali consumption and carbon dioxide emissions are reduced by 9.43 and 27.17%, respectively. This exploration provides a theoretical reference for the development application and industrial research of ED processes using IL-based mixed solvents.

1. INTRODUCTION

In the chemical industry, ethyl acetate (EtAc) is fast dried and nontoxic and is often used in coatings and paints, and because of its ester flavor, it is often used in the food processing field, second, it is an excellent chemical raw material, widely used in the production process of pharmaceuticals and fine chemicals.[1−3] Ethanol (EtOH) is mainly used for solvents, reaction media, fuel, and synthesis of other chemicals.[4] Under the conditions of acidic catalysts, EtAc is produced by esterification using EtOH with acetic acid, sometimes to increase the reaction rate, the amount of EtOH will be increased, so that the coboiling system of EtAc−EtOH will be generated in this process. Because the coboiling has a fixed boiling point, its gas phase composition is the same as the liquid phase composition, which makes the separation of two substances with high purity difficult.[5] The high-purity recovery of EtAc and EtOH can not only reduce resource waste but also reduce environmental pollution, while improving the added value of products, making the development of processes sustainable.[6] Therefore, achieving green and efficient separation of EtAc and EtOH has important practical significance.

Since EtOH dissolves in water, EtAc is hardly soluble in water. This property makes the solubility of EtAc in water very low, and it is difficult to separate it from EtOH with high purity

Received: April 5, 2024
Revised: May 11, 2024
Accepted: May 22, 2024
Published: June 5, 2024

© 2024 The Authors. Published by American Chemical Society

by simple extraction methods, EtAc easily hydrolyzes to produce acetic acid and ethanol under alkaline conditions, so strong alkalis such as sodium hydroxide cannot be used for separation. In addition, the boiling points of EtAc and EtOH are relatively close to each other, which makes it difficult to separate them by separation techniques prevalent in chemical production.[6] Therefore, to effectively separate EtAc and EtOH, the commonly used coboiling separation methods mainly include pressure swing distillation (PSD), azeotrope distillation (AD), extractive distillation (ED), and so on.[7−9] Due to the characteristic that the azeotropic point changes significantly with pressure, PSD takes advantage of this feature and uses distillation columns with different operating pressures to achieve azeotropic separation. The principle is based on the pressure sensitivity of the azeotropic mixture system and does not require the addition of additional components compared to other methods.

AD forms an azeotrope with one or more components in the system by incorporating an external solvent, altering the relative volatility between mixtures, and achieving azeotropic separation. However, the inclusion of an entertainer escalates both the cost and complexity of the purification process. Simultaneously, the selection of the entrainer is pivotal to the separation outcome, necessitating a comprehensive evaluation of its selectivity, solubility, volatility, stability, and economic viability.[10] Conversely, ED combines extraction and distillation methods to isolate the lowest azeotrope. This is achieved by utilizing high boiling point solvents that do not produce new azeotropes in conjunction with the original mixed solution. While both ED and AD introduce an external solvent to augment relative volatility, unlike AD, the incorporated component in ED does not form an azeotrope with the component in the raw material. Furthermore, the extractant for ED exhibits a broad selectivity range and low consumption.[11] In practical applications, it is imperative to select suitable operating conditions and extractants based on specific circumstances. In conclusion, due to its merits such as high efficiency, energy conservation, and extensive applicability, ED is presently the predominant method for azeotropic separation. Moreover, there exists potential for further exploration and development of environmentally friendly, sustainable, and efficient ED technology, which holds vast application prospects.

ED has been widely studied by numerous scholars in the field of azeotropic separation. Cui et al.[12] established conventional and thermally integrated ED processes to optimize the process through Genetic Algorithms (GA) to increase the profit space of the process. Xin et al.[13] screened suitable ILs for separating the EtAc−EtOH azeotrope system through software, measured the isobaric gas−liquid phase equilibrium data of the ILs ternary system at atmospheric pressure, and expanded the simulation through software. In addition, this team also separated with tributylmethylammonium acetate as an extractant and quasi measurement reached the minimum usage amount for separation. Tsai et al.[14] introduced a new method for the initial design of bioethanol dehydration combining process fluctuation, which differs from previous studies that ignored fluctuations, and determined the feasible operating range of the process by considering fluctuations, increasing the flexibility of operation, providing valuable insights into the industrial application of ED for bioethanol dehydration. Czarnecki et al.[15] reviewed key aspects such as the design scheme of extraction and dividing wall column obtained by combining ED with denuder wall column, the selection process of entrainment, the simulation design method, and the control scheme. Cui et al.[16] achieved high-purity ethyl acetate and isopropanol recovery by triple ED treatment of pharmaceutical wastewater containing ethyl acetate/isopropanol/water.

The aforementioned optimization processes for ED predominantly employ the sequential iteration method. This approach is heavily reliant on the initial values of decision variables and is prone to becoming entrapped in local optimal solutions, resulting in suboptimal convergence for nonconvex optimization problems characterized by pronounced nonlinearity, such as those associated with the distillation column balance MESH equation group and phase equilibrium equation. In contrast, stochastic algorithms, including particle swarm and GA, are better equipped to address these challenges. Yang et al. optimized the separation process of EtAc−MeOH using multiobjective particle swarm optimization, considering annual total cost, CO_2 emission volume, and process route index as objectives.[17] Similarly, He et al. introduced an NSGA-II algorithm grounded in multiobjective optimization, with the primary objective of identifying Pareto optimal solutions.[18]

Organic solvents can promote high-purity separation. However, due to its inherent volatility, a certain degree of residue will lead to product contamination. On the other hand, ILs are known for its difficulty in volatilization, and large-scale application is both expensive and challenging.[19,20] In this research, we utilized computer-aided screening of solvents, and explored the mechanism of intermolecular interaction, and further screened suitable solvents based on it. Moreover, combining these two solvents to play their respective advantages was considered, while genetic algorithm was used for global optimization to avoid local optimal solution. Finally, when the mixed solvent extraction separation process was combined with heat pump technology, waste heat could be effectively utilized to reduce energy consumption. This not only improves economic benefits but also improves environmental protection,[21] and finally its potential application and value were evaluated through economic and environmental assessment.

2. SCREENING OF MIXED SOLVENTS AND MECHANISM ANALYSIS

2.1. Screening of Organic Solvents. In this study, we selected the optimal organic solvent by considering five commonly used solvents: dimethyl sulfoxide (organic solvent dimethyl sulfoxide (DMSO)), ethylene glycol (EG), *N*,*N*-dimethylformamide (DMF), ananol (ANOL), and methylparaben (MPH). These were chosen as candidate entrainers based on prior literature.[22−25] We examined the impact of these organic solvents on the vapor−liquid equilibrium (VLE) of the EtAc−EtOH system using Aspen Plus process simulation software, as depicted in Figure 1. The figure clearly shows that DMSO deviated more significantly from the diagonal line than other solvents under identical feed ratios. This deviation had a substantial effect on the VLE data for EtAc suggesting that DMSO has a more pronounced influence on the relative volatility of the azeotropic system. Consequently, DMSO was chosen as the organic extraction solvent for this study.

2.2. ILs Screening Based on the COSMO-RS Model. In the screening work of ILs, the selectivity of various ILs to the EtAc−EtOH system was studied by using the COSMO-RS

https://doi.org/10.1021/acsomega.4c03270
ACS Omega 2024, 9, 26596−26606

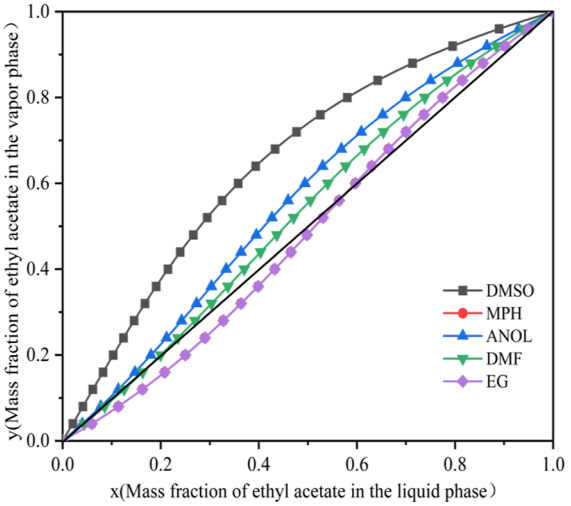

Figure 1. Effect of different organic solvents on VLE data of EtAc−EtOH system.

model,[26,27] as shown in Figure 2, where the horizontal and vertical axis represents the anion and cation, respectively, and the intersection point of the perpendicular line of each axis represents the ILs. It is found that imidazole and pyridine are better selected for the cation, while acetate $[Ac]^-$, aminoacetic acid $[Gly]^-$ are better selected for the anion through image analysis. In practice, anion $[Ac]^-$ is more common than $[Gly]^-$, so it is appropriate to select $[Ac]^-$.

Although pyridinic ILs have low viscosity and high chemical stability, which are suitable solvents and catalysts for many reactions,[28,29] pyridinic ILs are complicated in the preparation process, poor thermal stability, and not advantageous in price (Price source: Monieres Chemical Engineering Science and Technology (Shanghai) Co., Ltd). Imidazolium-based ILs have higher electrical conductivity and thermal stability, wide applications in separation technology, gas absorption and electrochemistry, and relatively mature synthesis technology and low price, so the imidazolium-based ILs were selected to extract the EtAc−EtOH system by distillation. Some researchers reviewed and compared the separation research of typical low-carbon alcohol ester coevaporative systems containing ILs. It was found that common alkyl-substituted imidazolium cations did not contribute much to the change of relative volatility of coevaporates, while polar anions played a decisive role, which verified that alkyl-substituted imidazolium cations and polar anion-like ILs can effectively change the results of the relative volatility of alcohol ester coevaporative mixtures.[30] Combined with the above analysis, it was decided to select imidazolium cations and some anions as candidates for ILs, and then explore the molecular action mechanism to screen further.

2.3. Quantum Chemistry-Based ILs Screening. Calculation of σ-profile using the COSMO-RS module in the commercial software Amsterdam Modeling Suite 2022.103 licensed from Fermi Technology (Beijing) Co., Ltd.[31,32] The σ-profile spectrum shows the probability curve of the surface charge density of a substance, which characterizes the charge distribution and polarity of molecules. The two straight lines with e = ± 0.0082 Å^2 in the σ-profile diagram are divided into three regions, namely the hydrogen bond donor (HBD) region, hydrogen bond acceptor (HBA) region, and nonpolar region.[33] In the HBD domain ($\sigma \leq -0.0082$ e/Å^2), the closer to the left side of the peak position indicates that the molecule donor hydrogen has a stronger ability. Similarly, in the HBA region, the closer to the right side of the peak position, the molecule accepts hydrogen has a stronger ability. Combined with Figure 3a,b, the reason why EtAc and EtOH systems produce an azeotropic phenomenon is that EtOH has a strong ability to provide hydrogen bonds and ethyl acetate has a strong ability to receive hydrogen bonds, both combine to form a stronger molecular bond. The surface charge density region of EtOH and DMSO extends from the HBD area through the nonpolar area to the HBA area, on the surface this substance can be used as both acceptor and donor. The σ of EtOH reaches −0.017 e/Å^2 in the system and has the strongest ability to provide hydrogen bonds. Figure 3a shows the charge density probability distribution of imidazolium cations, the

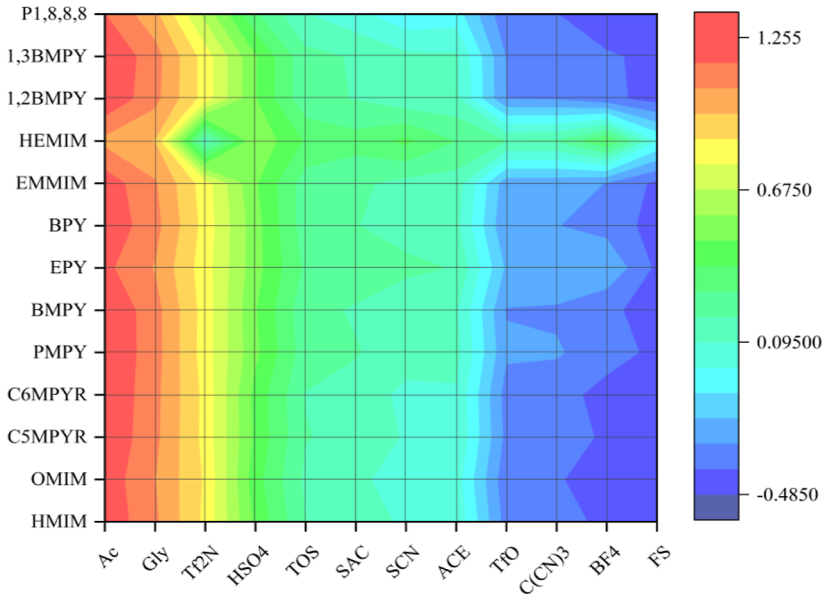

Figure 2. Selectivity values of EtAc−EtOH for different ILs at 298.15 K.

https://doi.org/10.1021/acsomega.4c03270
ACS Omega 2024, 9, 26596−26606

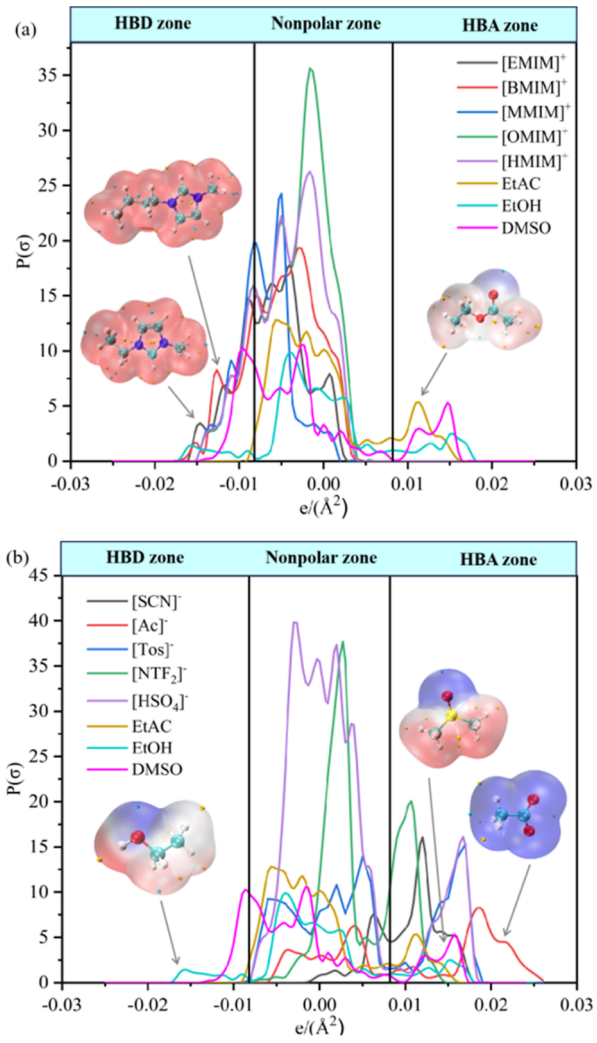

Figure 3. σ-Profile plots of EtAc, EtOH, DMSO, and polar anions and cations, (a) cations, (b) anions.

cations are mainly providers of hydrogen bonds and have similar providing abilities, in HBD region, $[BMIM]^+$ and $[EMIM]^+$ are relatively far away from line $\sigma = -0.0082$ e/Å^2, preliminary select easily synthesized $[BMIM]^+$ and $[EMIM]^+$ as cations of ILs. From Figure 3b polar anion mainly does HBA, through the figure found that the σ of acetate anion reached an astonishing 0.026 e/Å^2, compared with other anions that have very large polarity, which shows it has a stronger ability to receive hydrogen bond, so choose $[Ac]^-$ as anion of ILs. In the separation process, EtOH provides a strong hydrogen bond, and DMSO and anions of ILs combined break its interaction with EtAc, thus making the two substances separate. Overall, organic solvent DMSO, ILs [BMIM][Ac], and [EMIM][Ac] have great potential for separation of the coboiling system.

In addition, the σ-profile spectrum was supplemented by drawing an electrostatic potential distribution map (ESP map) of the molecular van der Waals surface. The red area represents ESP's positive values, and the blue area represents the negative values of ESP. By analyzing the charge distribution on the molecular surface, not only can its mechanism be further analyzed but also it can be inferred to speculate the reaction sites for material binding.[34] Through the analysis of the ESP map, the negative value (or minimum value) of EtOH is mainly concentrated near the oxygen of the hydroxyl group, and the positive value (or maximum value) is mainly concentrated near the hydrogen of a hydroxyl group. The minimum value of EtAc is concentrated around the double bond oxygen of the ester group, this point has a potential energy that can form a hydrogen bond with the hydrogen of a hydroxyl group of EtOH, which is consistent with the above analysis. Finally, we can also observe that both $[BMIM]^+$ and $[EMIM]^+$ have red ESP areas, points are all distributed around the imidazole ring, and the value is largest near the alkyl chain close to the imidazole ring, while $[Ac]^-$ has a blue ESP area, and the minimum value is located above the oxygen atom. Through analysis, in this system, anions play a major role in separation, as anion is added, the polarity of ILs is improved.[35] Therefore, strong polar molecules can produce stronger intermolecular forces and thus break the coboiling effect well when forming a firm complex with EtOH. Longer alkyl side chains will lead to higher viscosity and solubility. When considering the influence of the viscosity of ILs on industrial applications and the solubility of ILs, we determined [EMIM][Ac] as the ILs studied in this paper.

2.4. Energy of Interaction Analysis. The interaction energy can be used to explore the binding action and degree of separation between azeotropic liquids and various solvents. In this study, the molecules 1.1.2[36] program was used for molecular or atomic cluster configuration searches to find the most stable conformation at the same functional and basis set level. The quantum chemical program ORCA 5.0.3[37] was then used to perform preliminary optimization and frequency analysis and energy calculation on the initial structure of each component and mixture after dispersion correction based on the theoretical basis of B3LYP/6-31G*, calculate single-point energy of molecules without imaginary frequencies at a higher computational accuracy level of M062X/def2-TZVP, and correct dispersion. When performing quantum chemical calculations, due to the finiteness of the basis set, especially low group sets, it cannot perfectly describe the characteristics of real electron orbitals, resulting in the generation of basis set overlap errors, which will have a certain impact on the results, so that overlap errors should be eliminated when calculating single-point energy.[38] Its minimum interaction energy is calculated by the following formula

$$\Delta E = 2625.5 \times (E_{AB} - E_A - E_B + E_{BSSE}) \quad (1)$$

The larger the modulus of interaction energy, the stronger the intermolecular interaction. ΔE in eq 1 is the interaction energy; E_A and E_B represent the energy of substances A and B; E_{AB} is the energy of two molecular composite structures (A−B); E_{BSSE} is the correction energy caused by molecular overlap.

As shown in Table 1, the interaction energies of organic solvents or ILs with the coevaporating system were all greater than those of pure components. In addition, the single point energy of [EMIM][Ac] was significantly higher than that of DMSO, indicating that the extractive effect of ILs was better than that of organic solvent, meaning that the same extractive effect could be achieved with a smaller amount of extractant. By calculating the interaction energy between each extractant and each component of the system, it was found that all extractants were firmly bound to EtOH, which made EtAc separate first. This result is consistent with the previous analysis.

2.5. Independent Gradient Model Analysis. The section adopts the IGM method based on Hirshfeld partition

https://doi.org/10.1021/acsomega.4c03270
ACS Omega 2024, 9, 26596−26606

Table 1. Interfacial Energy between Components and Solvents

A	B	E_{AB} (kJ/mol)	E_{bsse} (kJ/mol)	ΔE (kJ/mol)
EtAc	EtOH	−1215032.83	2.39	−44.98
EtAc−EtOH	DMSO	−2667526.00	4.87	−61.07
EtAc−EtOH	[EMIM][Ac]	−2720194.40	3.69	−87.44
DMSO	EtAc	−2260405.26	2.39	−51.16
	EtOH	−1859547.31	2.39	−58.24
[EMIM][Ac]	EtAc	−2313109.29	4.24	−75.09
	EtOH	−1912254.71	4.51	−85.20

of molecular density (IGMH),[39] visualize the interaction forces between solvent DMSO, [EMIM][Ac] and EtAc−EtOH molecules based on Multiwfn 3.8[40] and VMD 1.9.1[41] software, maps the functional color contrast diagram as well as the atomic schematic diagram are shown in Figure 4.

The $g^{IGM,inter}$ isosurface plot of sign$(\lambda^2)\rho$ for DMSO, [EMIM][Ac], and EtAc−EtOH systems are shown in Figure 5. It can be found that the isosurface of EtAc−EtOH system is blue-green, and there are hydrogen bonds or van der Waals (vdw) on the surface, which also reveals the reason why this system produces coevaporation. Further analysis shows that the two combine to form the highest peak in the corresponding scatter plot, i.e., sign$(\lambda^2)\rho \approx -0.028$ au and $g^{IGM,\ inter} \approx 0.077$ au, they form O−H···O type hydrogen bond on the surface, hydroxyl oxygen and hydrogen of ester mainly form vdw, oxygen atom in ester group and hydrogen atom of alkyl chain form weak dispersion force. Figure 5b shows the $g^{IGM,\ inter}$ isosurface plot of sign$(\lambda^2)\rho$ for organic solvent DMSO and coevaporating system EtAc−EtOH, specifically, the oxygen atom in DMSO and hydroxyl hydrogen in EtOH form very thick blue isosurface filling plane on the surface, then they form the highest peak in the scatter plot, i.e., sign$(\lambda^2)\rho \approx -0.032$ au and $g^{IGM,inter} \approx 0.074$ au, while the hydroxyl oxygen atom of EtOH and hydrogen atom in DMSO form a pan-blue green isosurface at sign$(\lambda^2)\rho \approx -0.014$ au and $g^{IGM,inter} \approx 0.035$ au, its interaction force is weaker than the former but belongs to C−O···H type hydrogen bond with stronger interaction. The rest part is green isosurface, among them the green isosurface formed by the hydrogen atom of EtAc and sulfur atom in DMSO has the largest area, meaning that the combination of solvent and EtOH is more solid than EtAc, which is consistent with the previous analysis. Figure 5c shows the isosurface plot of the azeotropic system and the IL, the hydrogen atom of EtAc forms a green isosurface with imidazole ring, i.e., vdW; $[Ac]^-$ oxygen atom in it forms C−O···H type hydrogen bond with alkyl hydrogen of EtOH, the hydrogen atom in $[EMIM]^+$ alkyl chain forms C−O···H type hydrogen bond with the oxygen atom of EtOH, the peak width in the scatter plot is wider than that of DMSO, so its combination effect is stronger than that of organic solvents.

3. EVALUATION ANALYSIS

3.1. Economic Evaluation. The economic evaluation criteria for process design encompass the TAC ($/year), which encompasses both equipment cost (ACC) and operating cost (AOC). The ACC primarily refers to the annual calculation of distillation column and heat exchanger costs, with the plant's operational duration typically serving as the benchmark. It is presumed that the plant has been in operation for three years, equivalent to 8000 h.[42] The AOC primarily encompasses the utility engineering costs, including steam and cooling water expenses. In conducting this economic evaluation, the paper utilizes the Douglas economic model and the previously optimized process flow.[43] The specific calculation method is detailed in S3, and its comprehensive representation is as follows

$$\mathrm{TAC} = \frac{\mathrm{ACC}}{3} + \mathrm{AOC} \tag{2}$$

3.2. Carbon Emissions Assessment. As one of the key greenhouse gases, the emission of large amounts of CO_2 will aggravate global warming, highlighting the urgency to control emissions. In response to this challenge, countries have formulated and implemented corresponding policies. Among various separation processes, the energy required for distillation columns and their heat exchange networks mainly comes from the combustion of fossil fuels such as oil, natural gas, and coal.[44] Therefore, reducing the energy consumption of the distillation separation process not only means reducing the TAC but also helps to reduce greenhouse gas emissions, which greatly improves the sustainability of production. Assuming that air is excess and does not produce CO, the amount of CO_2 emissions (kg/h) is calculated by[45]

$$m_{co_2} = \left(\frac{Q_{\mathrm{Fuel}}}{\mathrm{NHV}}\right)\left(\frac{C\ \%}{100}\right)\alpha \tag{3}$$

In the given formula, Q_{Fuel} represents the total heat released from fuel combustion (in kilowatts). C % denotes the carbon content in the fuel. Net heating value (NHV) signifies the net calorific value of unit mass fuel combustion. The ratio of the molar molecular mass of CO_2 to C_{12} is denoted by α, with a

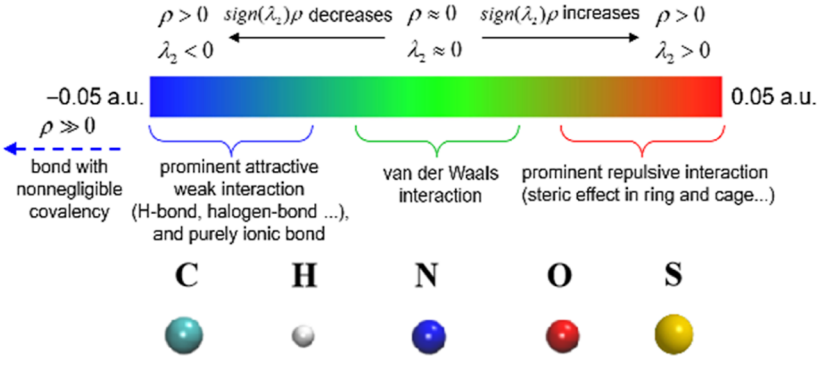

Figure 4. Color comparison and atomic schematic of mapping functions in IGMH.

https://doi.org/10.1021/acsomega.4c03270
ACS Omega 2024, 9, 26596−26606

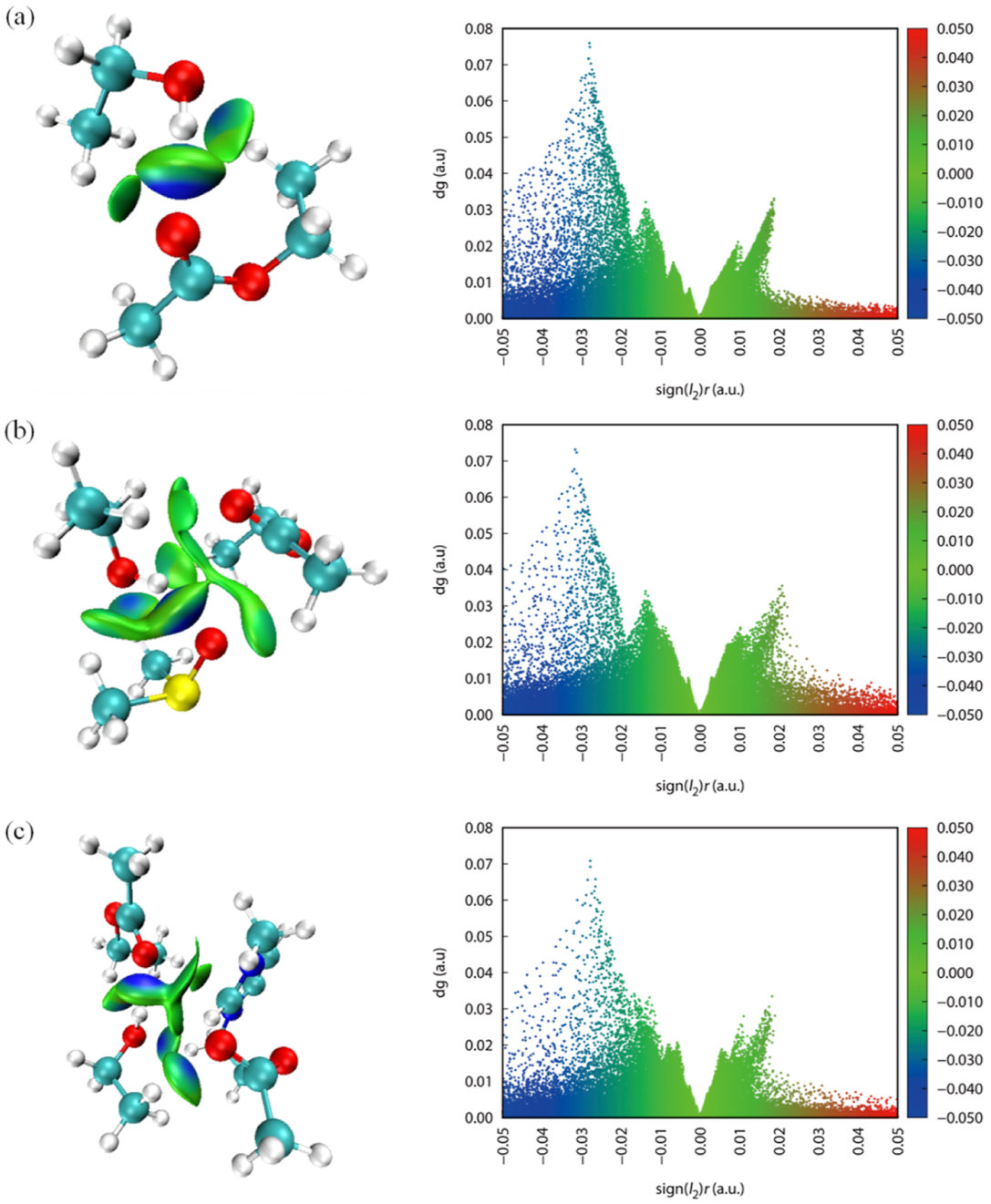

Figure 5. Isosurfaces of $g^{IGM,inter}$ colored by sign(λ^2)ρ between solvent and azeotrope molecules: (a) EtAc−EtOH, (b) EtAc−EtOH and DMSO, (c) EtAc−EtOH and [EMIM][Ac].

specific value of 3.67. In distillation systems, superheated steam is frequently employed as either an indirect heating medium or a direct stripping medium. This steam is typically produced by combusting fuel in a boiler. For the sake of analytical simplicity, we assume that coal is used to generate steam, with its NHV and carbon content (C %) values being 22,000 kJ/kg and 68.0%, respectively. The quantity of fuel (Q_{Fuel}) is then calculated using the following formula

$$Q_{Fuel} = \frac{Q_R}{\eta_{Fuel}} \quad (4)$$

Q_R is the reboiler heat load, η_{Fuel} is the heating efficiency, generally 0.8−0.9, and this paper takes 0.8.

4. SEPARATION PROCESS SIMULATION AND OPTIMIZATION

4.1. UNIFAC-Lei Modeling. The mixed extractant extractive process of the EtAc−EtOH azeotropic system was simulated using the RadFrac module in the process simulation software. This allowed for a comparison of the separation effects of various mixed extractants on a system scale. ILs, as an emerging class of substances with numerous types, lack many physical parameters. However, Lei et al.[46−48] developed the UNIFAC-Lei model based on the UNIFAC thermodynamic model for ILs. This model is extensively utilized to predict liquid−liquid, vapor−liquid, and other thermodynamic equilibrium data. Binary interaction parameters necessary for simulation were defined based on this model. For further

https://doi.org/10.1021/acsomega.4c03270
ACS Omega 2024, 9, 26596−26606

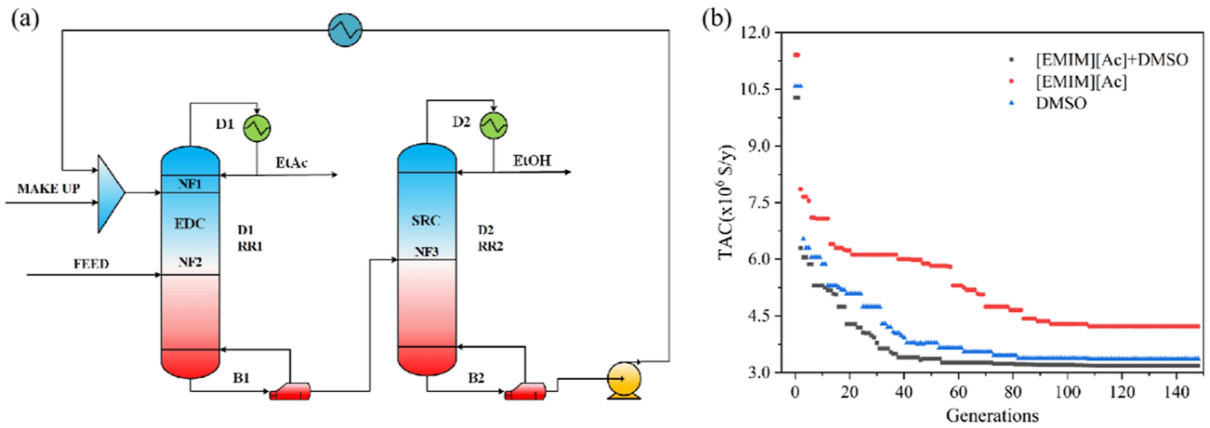

Figure 6. ED process flowchart and optimization results for separating EtAc and EtOH, (a) process flowchart, (b) optimal solution per generation of the algorithm.

reference, the Supporting Information S4−S7 provide the necessary data for this simulation.

4.2. ED Process Simulation. This study is targeted at the separation process of EtAc−EtOH system by double-tower mode, namely ED column (EDC) and solvent recovery column (SRC). The azeotropic mixture enters from the middle part of EDC with an azeotropic composition, and the extractant enters from the upper part of the tower. After the extraction operation, the pure light component is taken out at the top of the tower, and the extractant and recombined components are taken out in the column. For the recovery of extractants, flash evaporation technology, supercritical extraction technology, distillation technology, and other conventional methods can be adopted.[49−51] Considering the composition of the ILs composite extractant proposed in this paper, distillation technology can be selected to recover the extractant. The simulation conditions are as follows: feed flow rate of raw material is 200 kmol/h, operating temperature and pressure are 298.15 K, 1 atm, respectively, where the molar content of EtAc is 0.54, and the purity of separation product is required to be above 99.5%. Taking the purity of EtAc and EtOH at the top of the tower meets the condition as a premise, optimization of the whole process is carried out with minimum TAC as a target. The ED process flowcharts of organic solvent, ILs, and mixed solvent are shown in Figure 6a.

The optimization of the ED process is formulated as a complex mixed-integer nonlinear programming (MINLP) problem.[52] Typically, to solve MINLP problems, one can either utilize deterministic global optimization methods or stochastic global optimization methods.[53] While deterministic optimization algorithms can yield strictly global optimal solutions, they are often time-consuming and computationally expensive for highly nonlinear and variable number ED optimization processes. Conversely, stochastic global optimization methods can identify feasible approximate optimal solutions within a reasonable computation time frame. Given that GA exhibit high parallelizability, this study employs GA for stochastic optimization.[54] The optimization process is executed on Aspen Plus V14.0 using Python 3.9 software. The stopping criterion for GA is set at the point where the optimal value remains unchanged for 30 consecutive generations.

The optimal solution for each generation of the process described in this paper is shown in Figure 6b.

In picture 6 and Table 2, NT1 and NT2 represent the total number of trays for tower EDC and tower SRC, respectively; RR1 and RR2 represent the reflux ratio of tower EDC and tower SRC, respectively; NF1 and NF2 represent the extractant feed tray position and mixed material feed tray position of tower EDC, respectively; NF3 is the feed position of tower SRC.

Table 2. Optimization Parameters and Results of Each Extractive Process

parameter	DMSO	[EMIM][Ac]	[EMIM][Ac]+DMSO
feed flow rate (kmol/h)	402	462	438
NT1	25	30	24
NT2	15	15	15
NF1	4	2	3
NF2	17	21	15
NF3	12	5	11
RR1	0.84	3.12	1.7
RR2	0.49	0.15	0.22
D1(m)	1.57	1.92	1.67
D2(m)	1.00	1.57	1.01
make-up (kmol/h)	0.31	0.02	3.8×10^{-5}
total heat load (kW)	9177	11,810	9656
TAC ($*10^6$ $/y)	3.3564	4.4226	3.1852

Given the same feed quantity and the objective of accomplishing an identical separation task, the ED separation process was optimized using a genetic algorithm program. The optimization outcomes for the three processes are summarized in Table 2.

Software simulations have demonstrated that the organic solvent DMSO and [EMIM][Ac] can be effectively utilized in the ED separation process. The loss of organic solvent is the most significant, whereas both [EMIM][Ac] exhibit high saturation vapor pressures, resulting in relatively minor losses. Furthermore, the quantity of extractant required for the mixed solvent ED separation process is minimal, with a smaller loss from the mixture of organic solvent and ILs. This suggests that employing ILs in the separation process yields a higher recovery rate of extractant. The second ILs extractive effect is notably significant, requiring fewer quantities to achieve equivalent extractive results, thereby reducing energy consumption in chemical engineering equipment. The mixed solvent extractive process warrants further consideration, particularly in terms of economic efficiency and environmental impact. Although the separation efficacy of ILs generally

https://doi.org/10.1021/acsomega.4c03270
ACS Omega 2024, 9, 26596−26606

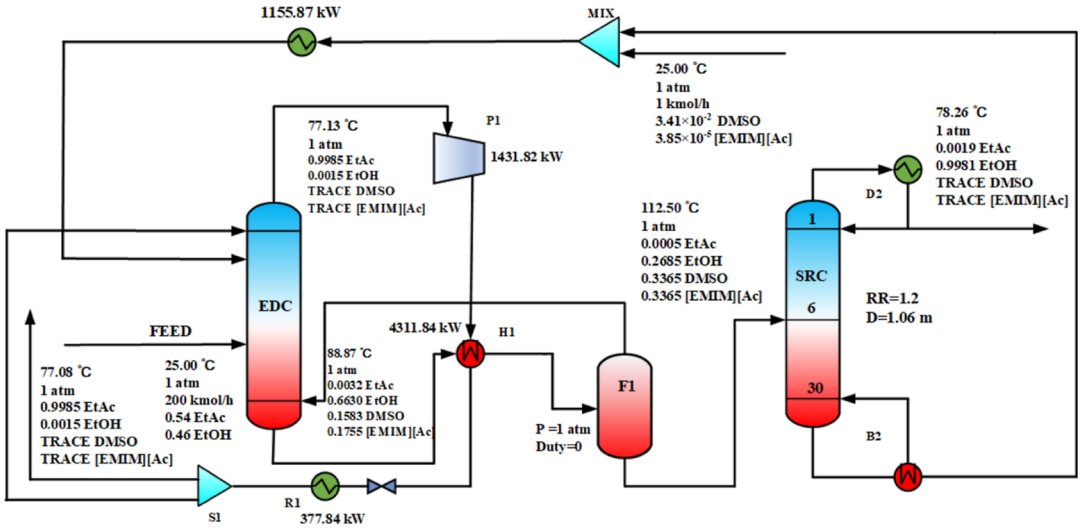

Figure 7. Flowchart of vapor recompression-assisted ED separation process for composite extractive solvents.

surpasses that of traditional organic solvents, its higher boiling point leads to an increase in reboiler heat load, consequently raising energy consumption and economic costs. IL-based mixed solvents represent a product that balances economic consumption with separation effectiveness.

4.3. Vapor Recompression Assisted ED Process Enhancement. The vapor recompression process (VRED) is an energy-efficient technology that utilizes its own secondary steam to pass through a compressor, thereby augmenting the heat to satisfy the heat demand of the reboiler and consequently reducing the need for external energy.[55] If the heat flow of EDC can preheat the feed stream, it will significantly reduce the heat loss of the flow and subsequently decrease the thermal load on the distillation column. Consequently, the feed preheating process is initially employed to diminish the energy consumption of ED, thereby minimizing energy and entropy losses. This approach has led to the widespread use of bubble point feed in industry for energy conservation and process stability. Building upon the previous mixed solvent ED process, this paper presents a process design as illustrated in Figure 7. The paper suggests that after exchanging the steam at the top of EDC for heat, the compressed air flow is compressed by a compressor to enhance the thermal grade of the air flow. This heat flow serves as a source to warm the air flow at the base of EDC, exchanging heat with the compressed heat flow. However, some of the steam at the bottom of EDC fails to meet separation requirements, necessitating the addition of an auxiliary reboiler H1. Following heat exchange, since the compressed heat flow has not been entirely liquefied, it requires condensation; hence, a condensater R1 is incorporated.

Figure 8 illustrates the temperature-enthalpy (T-H) diagram of the VRED process, serving as a tool to assess the thermal integral feasibility of the procedure. The red curve in Figure 8 represents the heat composite curve (HCC), while the blue curve denotes the cold composite curve (CCC). The displacement of HCC signifies all heat flows and equipment necessitating cooling, thereby representing the demand for cooling facilities (Q_{CW}), inclusive of the condenser load within the current process. In contrast, the displacement of CCC (Q_H) symbolizes the total heat demand in the process, specifically, the reboiler load within this process. Both curves in

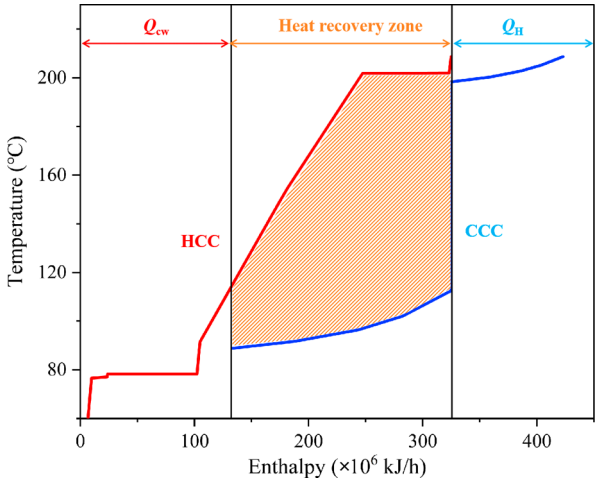

Figure 8. T-H diagram of vapor recompression-assisted ED separation process for composite extractive solvents.

the figure are constructed by integrating every interval temperature corresponding to either heat flow or cold flow. The overlap area between both curves, represented by the dashed line area, indicates the recovery of heat in the process (1.9134×10^8 kJ/h). Notably, a larger overlap area suggests a more comprehensive heat recovery.

5. EVALUATIONS AND ANALYSIS

Figure 9 provides a comprehensive overview of the cost and carbon emission outcomes associated with various extractive processes. Using an IL-based mixed solvent process compared with pure organic solvent and pure ILs separation processes, TAC decreased by 5.11 and 27.98%, respectively, and CO_2 emissions from the mixed solvent process were slightly higher than those from the organic solvent process. But the ILs mixed extractant process could make the extractant loss reduced, which undoubtedly can save a sum of extractant costs. For the ED process, waste heat generated by fluids and other factors was not fully utilized. By improving the process, waste heat can be effectively recycled, and compared with previous processes, utility engineering, TAC, and carbon emissions were reduced by 9.43, 27.17%. Generally, pure ILs as an extractant did not

https://doi.org/10.1021/acsomega.4c03270
ACS Omega 2024, 9, 26596−26606

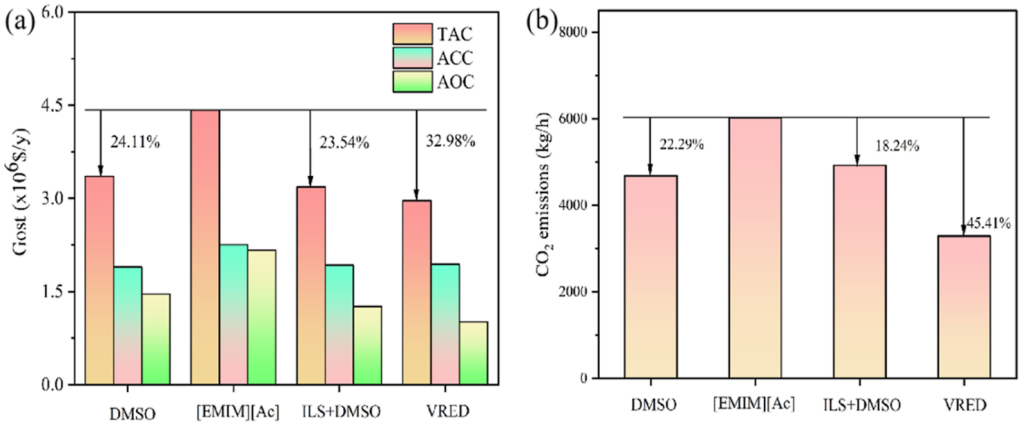

Figure 9. Comparison of parameters of different processes (a) Economy, (b) Carbon emissions.

yield the anticipated benefits in terms of process economy and environmental performance when compared to dimethyl sulfoxide. However, mixed solvents demonstrated superior economic and environmental performance. The extractive process using dimethyl sulfoxide was less efficient than that using ILs, necessitating a substantial amount of extractant raw material for successful ED separation. Despite the minor usage of ILs, its high viscosity and strong interaction force with the coboiling component led to increased operating costs. Mixed solvents mitigate this issue, albeit with slightly higher energy consumption than organic solvent processes. However, from an economic standpoint, they offer significant advantages. Furthermore, it was observed that the reflux ratio positively correlated with the heat load of the distillation column. Consequently, an increase in heat load would result in higher utility engineering costs and TAC. Given that thermal power generation is China's primary energy source, coal combustion remains the main source of carbon emissions. Therefore, minimizing energy consumption is vital for environmental sustainability. It should be emphasized that enhancing the composite extractant process can significantly reduce carbon emissions by utilizing waste heat, thereby saving a considerable portion of operating costs. This makes the improved process highly promising for engineering applications.

6. CONCLUSIONS

In this study, the organic solvent DMSO and a series of ILs were evaluated using computer-aided simulation to screen out [EMIM][Ac], and the mechanism of action was elucidated. The binding sites of multiple molecules were determined by ESP, while interaction energy analysis was used to evaluate the binding ability of various systems. The bond strength between molecules was visualized using IGMH analysis. Surface ILs showed greater forces than organic solvents, indicating that they may produce better results in the ED separation process. To confirm this finding, simulation results based on the UNIFAC-Lei model showed that the extractive effect was consistent with molecular mechanism analysis. Notably, during the extractive process of mixed solvents, there was little extractant loss, making it cost-effective and environmentally friendly. Steam-assisted heavy pressure processes improved the performance and feasibility of the production process. Compared with traditional solvents (DMSO), IL-based mixed solvents showed significant improvements in energy efficiency, environmental impact, and economic performance. Process simulation software revealed that both organic solvent and IL-based processes could satisfy the separation requirements. Subsequently, the separation process involving mixed solvents was scrutinized, with the three processes being globally optimized using GA. The combined ED process of the IL and organic solvent leveraged the benefits of both substances, thereby reducing solvent usage and operational costs associated with mass transfer and heat transfer. It was observed that prioritizing the separation process involving a mixture of solvents was more beneficial than focusing solely on the pure ILs extractive process or the pure organic solvent extractive process. Furthermore, the separation process involving a mixture of solvents exhibited marginally higher carbon emissions compared to the pure organic solvent, an improvement facilitated by the VRED process. This study demonstrated significant enhancements in both economic efficiency and carbon emissions, offering a theoretical foundation for future industrial applications.

■ ASSOCIATED CONTENT

Supporting Information

The Supporting Information is available free of charge at https://pubs.acs.org/doi/10.1021/acsomega.4c03270.

Provides IL physical properties, σ-profiles for all ions and molecules, UNIFAC action parameters for software simulations, and methods for economic evaluation and optimization of processes (PDF)

■ AUTHOR INFORMATION

Corresponding Author

Qiang Wang − *School of Chemical Engineering and Technology, Xinjiang University, Urumqi 830017 Xinjiang, China*; orcid.org/0000-0002-5248-6466; Email: wangqiang@xju.edu.cn

Authors

Jiajie Liu − *School of Chemical Engineering and Technology, Xinjiang University, Urumqi 830017 Xinjiang, China*; orcid.org/0009-0002-9405-6357

Yueran Yin − *School of Chemical Engineering and Technology, Xinjiang University, Urumqi 830017 Xinjiang, China*

Sijia Dai − *School of Chemistry and Chemical Engineering, Hainan University, Haikou 570228 Hainan, China*

Biao Liu − *School of Chemical Engineering and Technology, Xinjiang University, Urumqi 830017 Xinjiang, China*

Complete contact information is available at:

https://doi.org/10.1021/acsomega.4c03270
ACS Omega 2024, 9, 26596−26606

https://pubs.acs.org/10.1021/acsomega.4c03270

Notes

The authors declare no competing financial interest.

■ ACKNOWLEDGMENTS

We are grateful to Dr. Muhammad Furqan for the writing supervision of this manuscript.

■ REFERENCES

(1) Cheng, C.; Cong, Y.; Du, C.; Wang, J.; Yao, G.; Zhao, H. Solubility determination and thermodynamic models for dehydroepiandrosterone acetate in mixed solvents of (ethyl acetate + methanol), (ethyl acetate + ethanol) and (ethyl acetate + isopropanol). *J. Chem. Thermodyn.* **2016**, *101*, 372−379.
(2) Djojoputro, H.; Ismadji, S. Density and viscosity correlation for several common fragrance and flavor esters. *J. Chem. Eng. Data* **2005**, *50* (2), 727−731.
(3) Li, X.; Liu, Y.; Chen, J.; Chen, G.; Zhao, H. Preferential solvation of dehydroepiandrosterone acetate in (co-solvent + ethyl acetate) mixtures according to the inverse Kirkwood−Buff integrals method. *J. Chem. Thermodyn.* **2017**, *111*, 149−156.
(4) Saini, S.; Chandel, A. K.; Sharma, K. K. Past practices and current trends in the recovery and purification of first-generation ethanol: A learning curve for lignocellulosic ethanol. *J. Clean. Prod.* **2020**, *268*, 122357.
(5) Shen, W. F.; Benyounes, H.; Song, J. A review of ternary azeotropic mixtures advanced separation strategies. *Theor. Found. Chem. Eng.* **2016**, *50* (1), 28−40.
(6) Hasanoglu, A.; Salt, Y.; Keleser, S.; Ozkan, S.; Dincer, S. Pervaporation separation of ethyl acetate-ethanol binary mixtures using polydimethylsiloxane membranes. *Chem. Eng. Process* **2005**, *44* (3), 375−381.
(7) Wang, K.; Li, J.; Liu, P.; Lian, M. L.; Du, T. Z. Pressure swing distillation for the separation of methyl acetate-methanol azeotrope. *Asia-Pac. J. Chem. Eng.* **2019**, *14* (3), No. e2319.
(8) Li, J. W.; Lei, Z. G.; Ding, Z. W.; Li, C. Y.; Chen, B. H. Azeotropic distillation: A review of mathematical models. *Separ. Purif. Rev.* **2005**, *34* (1), 87−129.
(9) Lei, Z. G.; Li, C. Y.; Chen, B. H. Extractive distillation: A review. *Separ. Purif. Rev.* **2003**, *32* (2), 121−213.
(10) de Jong, M. C.; Zondervan, E.; Dimian, A. C.; de Haan, A. B. Entrainer selection for the synthesis of fatty acid esters by Entrainer-based Reactive Distillation. *Chem. Eng. Res. Des.* **2010**, *88* (1), 34−44.
(11) Kiss, A. A.; Suszwalak, D. J. P. C. Enhanced bioethanol dehydration by extractive and azeotropic distillation in dividing-wall columns. *Sep. Purif. Technol.* **2012**, *86*, 70−78.
(12) Cui, J.; Li, Z.; Xiao, H.; Pan, H.; Zhang, P.; Gui, P.; Yao, C.; Qi, L. Multi-Objective Optimization of Extractive Distillation and Heat-Integration Improvement Process for Acetonitrile and Water. *Acta Pet. Sin.* **2022**, *38* (5), 1135−1147.
(13) Xin, H. Study on Separation of Ethyl Acetate-Ethanol Azeotrope by Ionic Liquid Extractive Distillation. Master Degree, 2022.
(14) Tsai, C. Y.; Ang, T.; Kong, Z. Y.; Sunarso, J.; Adi, V. S. K. Toward a Flexible Design for the Bioethanol Dehydration Using Extractive Distillation. Part 1: Steady-State Design and Optimization. *Ind. Eng. Chem. Res.* **2023**, *62* (51), 22043−22057.
(15) Czarnecki, N. J.; Owens, S. A.; Eldridge, R. B. Extractive Dividing Wall Column for Separating Azeotropic Systems: A Review. *Ind. Eng. Chem. Res.* **2023**, *62* (14), 5750−5770.
(16) Cui, P. Z.; Zhao, F.; Yao, D.; Ma, Z. Y.; Li, S. H.; Li, X.; Wang, L.; Zhu, Z. Y.; Wang, Y. L.; Ma, Y. X.; Xu, D. M. Energy-Saving Exploration of Mixed Solvent Extractive Distillation Combined with Thermal Coupling or Heat Pump Technology for the Separation of an Azeotrope Containing Low-Carbon Alcohol. *Ind. Eng. Chem. Res.* **2020**, *59* (29), 13204−13219.
(17) Yang, A.; Ernawati, L.; Wang, M.; Kong, Z. Y.; Sunarso, J.; Sun, S.; Shen, W. Multi-objective optimization of the intensified extractive distillation with side-reboiler for the recovery of ethyl acetate and methanol from wastewater. *Sep. Purif. Technol.* **2023**, *310*, 123131.
(18) He, Q.; Li, Q.; Tan, Y.; Dong, L.; Feng, Z. Multi-objective optimization of sustainable extractive dividing-wall column process for separating methanol and trimethoxysilane azeotrope mixture. *Chem. Eng. Process* **2022**, *181*, 109141.
(19) Armand, M.; Endres, F.; MacFarlane, D. R.; Ohno, H.; Scrosati, B. Ionic-liquid materials for the electrochemical challenges of the future. *Nat. Mater.* **2009**, *8* (8), 621−629.
(20) Le Bideau, J.; Viau, L.; Vioux, A. Ionogels, ionic liquid-based hybrid materials. *Chem. Soc. Rev.* **2011**, *40* (2), 907−925.
(21) Chatel, G.; Pereira, J. F. B.; Debbeti, V.; Wang, H.; Rogers, R. D. Mixing ionic liquids - "simple mixtures" or "double salts"? *Green Chem.* **2014**, *16* (4), 2051−2083.
(22) Yang, S. K.; Wang, Y. J.; Bai, G. Y.; Zhu, Y. Design and Control of an Extractive Distillation System for Benzene/Acetonitrile Separation Using Dimethyl Sulfoxide as an Entrainer. *Ind. Eng. Chem. Res.* **2013**, *52* (36), 13102−13112.
(23) Dong, Y. C.; Dai, C. N.; Lei, Z. G. Extractive distillation of methylal/methanol mixture using ethylene glycol as entrainer. *Fluid Phase Equilib.* **2018**, *462*, 172−180.
(24) Yang, Q.; Xu, W.; Li, J.; Wang, Z.; Xu, H.; Zhou, M.; Wang, Y.; Li, X.; Zhong, L.; Cui, P. Molecular mechanism of efficient separation of isopropyl alcohol and isooctane by extractive distillation. *Chem. Eng. Res. Des.* **2024**, *204*, 269−281.
(25) Hu, C.; Cheng, S. Development of alternative methanol/dimethyl carbonate separation systems by extractive distillation - A holistic approach. *Chem. Eng. Res. Des.* **2017**, *127*, 189−214.
(26) Han, J.; Dai, C.; Yu, G. Q.; Lei, Z. Parameterization of COSMO-RS model for ionic liquids. *Green Energy Environ.* **2018**, *3* (3), 247−265.
(27) Khan, A.; Ibrahim, T.; Rashid, Z.; Khamis, M.; Nancarrow, P.; Jabbar, N. COSMO-RS based screening of ionic liquids for extraction of phenolic compounds from aqueous media. *J. Mol. Liq.* **2021**, *328*, 115387.
(28) Zhou, M.; Li, Y. Synthesis of 3;4-dihydropyrimidine-2(1H)-ones using ionic liquid butyl pyridinium tetrafluoroborate as a catalyst and medium , **2006**, *27* (3), 435−438.
(29) Ma, X.; Wei, J.; Guan, W.; Pan, Y.; Zheng, L.; Wu, Y.; Yang, J.-Z. Ionic parachor and its application to pyridinium-based ionic liquids of {[Cnpy] [DCA] (n = 2,3,4,5,6)}. *J. Chem. Thermodyn.* **2015**, *89*, 51−59.
(30) Zhang, L.; Wang, J.; Yang, L.; Xu, D.; Ma, Y.; Gao, J.; Wang, Y. Separation of isopropyl alcohol + isopropyl acetate azeotropic mixture: Selection of ionic liquids as entrainers and vapor−liquid equilibrium validation. *Chin. J. Chem. Eng.* **2022**, *50*, 326−334.
(31) Louwen, J. N.; Pye, C. C.; van Lenthe, E.; McGarrity, E. S.; Xiong, R.; Sandler, S. I.; Burnett, R. I.; *AMS202* COSMO-RS, SCM, Theoretical Chemistry*, Vrije Universiteit, Amsterdam, The Netherlands, URL: http://www.scm.com.
(32) Pye, C. C.; Ziegler, T.; van Lenthe, E.; Louwen, J. N. An implementation of the conductor-like screening model of solvation within the Amsterdam density functional package - Part II. COSMO for real solvents. *Can. J. Chem.* **2009**, *87* (7), 790−797.
(33) Zhu, Z.; Geng, X.; He, W.; Chen, C.; Wang, Y.; Gao, J. Computer-Aided Screening of Ionic Liquids As Entrainers for Separating Methyl Acetate and Methanol via Extractive Distillation. *Ind. Eng. Chem. Res.* **2018**, *57* (29), 9656−9664.
(34) Cvjetko Bubalo, M.; Radosevic, K.; Radojčić Redovniković, I.; Halambek, J.; Gaurina Srček, V. A brief overview of the potential environmental hazards of ionic liquids. *Ecotoxicol. Environ. Saf.* **2014**, *99*, 1−12.
(35) Cao, J. S.; Ren, Q.; Chen, F. W.; Lu, T. Comparative study on the methods for predicting the reactive site of nucleophilic reaction. *Sci. China Chem.* **2015**, *58* (12), 1845−1852.

https://doi.org/10.1021/acsomega.4c03270
ACS Omega 2024, 9, 26596−26606

(36) Qiao, Z.; Wu, Y.; Li, X.; Zhou, J. Molecular simulation on the separation of water/ethanol azeotropic mixture by poly (vinyl alcohol) membrane. *Fluid Phase Equilib.* **2011**, *302* (1−2), 14−20.
(37) Neese, F. *Software update: The ORCA program system—Version 5.0*; Wiley Interdisciplinary Reviews: Computational Molecular Science, 2022; Vol. *12*, p 1606.5
(38) Wang, C.; Zhuang, Y.; Dong, Y.; Zhang, L.; Liu, L.; Du, J. Design and control analysis of the side-stream extractive distillation column with low concentration intermediate-boiling entrainer. *Chem. Eng. Sci.* **2022**, *247*, 116915.
(39) Li, G.; Gui, C.; Zhu, R.; Lei, Z. Deep eutectic solvents for efficient capture of cyclohexane in volatile organic compounds: Thermodynamic and molecular mechanism. *AIChE J.* **2021**, *68* (3), 17535.
(40) Lu, T.; Chen, F. Multiwfn: a multifunctional wavefunction analyzer. *J. Comput. Chem.* **2012**, *33* (5), 580−592.
(41) Humphrey, W.; Dalke, A.; Schulten, K. VMD: visual molecular dynamics. *J. Mol. Graph.* **1996**, *14* (1), 33−38.
(42) Zhao, Q.; Shen, Y.; Li, Y.; Zhu, Z.; Cui, P.; Gao, J.; Ma, Y.; Wang, Y.; Wang, C. Process design and optimization of the efficient production of butyl acrylate by reactive azeotropic distillation/pervaporation using different feed ratios. *J. Clean. Prod.* **2022**, *344*, 131102.
(43) Chonghun, H.; Douglas, J. M.; Stephanopoulos, G. Agent-based approach to a design support system for the synthesis of continuous chemical processes. *Comput. Chem. Eng.* **1995**, *19*, 63−69.
(44) Kiss, A. A. Distillation technology-still young and full of breakthrough opportunities. *J. Chem. Technol. Biotechnol.* **2014**, *89* (4), 479−498.
(45) Gadalla, M. A.; Olujic, Z.; Jansens, P. J.; Jobson, M.; Smith, R. Reducing CO2 emissions and energy consumption of heat-integrated distillation systems. *Environ. Sci. Technol.* **2005**, *39* (17), 6860−6870.
(46) Dong, Y.; Dai, C.; Lei, Z. Separation of the Methanol−Ethanol−Water Mixture Using Ionic Liquid. *Ind. Eng. Chem. Res.* **2018**, *57* (32), 11167−11177.
(47) Dong, Y.; Dai, C.; Lei, Z. Extractive distillation of methylal/methanol mixture using ethylene glycol as entrainer. *Fluid Phase Equilib.* **2018**, *462*, 172−180.
(48) Zhu, R.; Kang, H.; Liu, Q.; Song, M.; Gui, C.; Li, G.; Lei, Z. UNIFAC Model for Ionic Liquids: 3. Revision and Extension. *Ind. Eng. Chem. Res.* **2024**, *63* (3), 1670−1679.
(49) Becerra, G.; Menolasina, S.; Salvador, A. Supercritical Fluid Extraction and Supercritical Fluid Chromatography of Vitamin E in Pharmaceutical Preparations. *J. High Resolut. Chromatogr.* **1999**, *22* (5), 300−302.
(50) Li, H.; Wu, Y.; Li, X.; Gao, X. State-of-the-Art of Advanced Distillation Technologies in China. *Chem. Eng. Technol.* **2016**, *39* (5), 815−833.
(51) Wang, C.; Xu, R.; Chen, X.; Jiang, P.; Liu, B. Study on water flash evaporation under reduced pressure. *Int. J. Heat Mass Transfer* **2019**, *131*, 31−40.
(52) Li, Q.; Tian, S.; Feng, Z.; Dong, L. Simulation and optimization for separation processes of methanol and trimethoxysilane azeotrope. *Chem. Ind. Eng. Prog.* **2021**, *40* (5), 2431−2439.
(53) An, W.; Hu, Y.; Yuan, X. Application and development of optimization techniques in distillation-based process synthesis. *Comput. Appl. Chem.* **2005**, *22* (5), 333−338.
(54) Cui, J.; Li, Z.; Xiao, H.; Pan, H.; Zhang, P.; Gui, P.; Yao, C.; Wei, L. Multi-Objective Optimization of Extractive Distillation and Heat-Integration Improvement Process for Acetonitrile and Water. *Acta Pet. Sin.* **2022**, *38* (5), 1135−1147.
(55) Zhang, Q.; Shi, P.; Zeng, A.; Ma, Y.; Yuan, X. Dynamic control analysis of intensified extractive distillation process with vapor recompression. *Sep. Purif. Technol.* **2020**, *233*, 116016.

https://doi.org/10.1021/acsomega.4c03270
ACS Omega 2024, 9, 26596−26606